Polymer Bulletin (2025) 82:1339–1355
https://doi.org/10.1007/s00289-024-05574-6

ORIGINAL PAPER

# Effect of the composition of block copolypeptides on their biocompatibility and anti-bacterial activities

**Ying-Jung Cheng[1] · Yi-Sheng Jiang[1] · Cheng-Rung Huang[2] · Chang-Shi Chen[2] · Jeng-Shiung Jan[1,3]**

Received: 2 October 2024 / Revised: 5 November 2024 / Accepted: 11 November 2024 /
Published online: 20 November 2024


## Abstract

The improper use of antibiotics in patients around the world increased the risk of multidrug-resistant bacterial infection and became a serious global health threat. Although many natural anti-bacterial peptides have been discovered, the low bioavailability of natural anti-bacterial peptides limited their therapeutic effect. Hence, it is necessary to develop customized synthetic anti-bacterial polypeptides. Poly(L-lysine) (PLL) is well-known to exhibit anti-bacterial properties. The tethering of hydrophobic peptide segments onto PLL might be able to improve not only the biocompatibility but also the anti-bacterial activity. The experimental data showed that the hydrophobic peptide segments played an important role in the biocompatibility and anti-bacterial activity of the block polypeptides. Among them, linear and 3-armed poly(L-lysine)-*block*-poly(L-alanine) block copolypeptides showed excellent biocompatibility and anti-bacterial activity against *Staphylococcus aureus* (*S. aureus*) and *Shigella flexneri* (*S. flexneri*). The in vivo experiments confirmed that the polypeptides could protect *Caenorhabditis elegans* (*C. elegans*) from bacterial infection, evidenced by the prolonged lifespan in the presence of polypeptides. Our results showed that these polypeptides could be potential candidates for treating bacterial infections.

**Keywords** Anti-bacterial peptide · Block copolypeptide · Peptide composition · *C. elegans*

## Abbreviations

| | |
|---|---|
| CD | Circular dichroism |
| *C. elegans* | *Caenorhabditis elegans* |
| FTIR | Fourier transform infrared |
| $IC_{50}$ | Half maximal inhibitory concentration |
| $M_n$ | Number-average molecular weights |

Ying-Jung Cheng and Yi-Sheng Jiang have contributed equally to this work.

Extended author information available on the last page of the article

| | |
|---|---|
| MIC | Minimum inhibitory concentration |
| NCAs | *N*-Carboxyanhydrides |
| NG | Nematode growth |
| PZLL | Poly(ε-benzyloxycarbonyl-L-lysine) |
| PLL | Poly(L-lysine) |
| Lys-Ala | Linear poly(L-lysine)-*block*-poly(L-alanine) |
| Lys-Leu | Linear poly(L-lysine)-*block*-poly(L-leucine) |
| Lys-Phe | Linear poly(L-lysine)-*block*-poly(L-phenylalanine) |
| 3s-Lys-Ala | 3-armed poly(L-lysine)-*block*-poly(L-alanine) |
| 3s-Lys-Leu | 3-armed poly(L-lysine)-*block*-poly(L-leucine) |
| 3s-Lys-Phe | 3-armed poly(L-lysine)-*block*-poly(L-phenylalanine) |
| RBCs | Red blood cells |
| ROP | Ring-opening polymerization |
| LB | Lysogeny broth |
| *S. aureus* | *Staphylococcus aureus* |
| *S. flexneri* | *Shigella flexneri* |
| TFA | Trifluoroacetic acid |
| THF | Tetrahydrofuran |
| TREN | Tris(2-aminoethyl)amine |
| ZLL | Z-L-lysine |

## Introduction

The impact of antibiotic-resistant bacterial strains should not be underestimated [1]. These strains have the potential to cause severe infections that are difficult to treat with conventional antibiotics. They pose a significant threat to public health and have led to an increased mortality rate worldwide. For instance, the cost for treatment of implant-associated osteomyelitis in the US is expected to exceed $1.62 billion by 2020 [2, 3]. Therefore, scientists around the world are dedicating their efforts to develop anti-bacterial biomaterials, which have become a top priority in the field of biomedical research in recent years [4]. The goal was to create materials that not only inhibit bacterial growth but also prevent the development of resistance over time. In addition to their anti-bacterial activity, anti-bacterial biomaterials must also be biocompatible with the human body. Previous studies have shown that the anti-bacterial activity of nature polypeptides was due to their peptide chains containing cationic and hydrophobic residues, enabling interactions with the cell membrane through electrostatic interactions, thereby disrupting bacterial morphology [5, 6]. These polypeptides hold the potential to revolutionize the field of medicine by providing new tools to combat bacterial infections. Therefore, the development of effective anti-bacterial polypeptides was crucial in addressing the escalating threat of antibiotic-resistant bacterial strains.

The design and synthesis of anti-bacterial polypeptides that mimic natural anti-bacterial peptides was one possible approach to overcome the limitation [6, 7]. This mostly thanks to great advances in synthesizing well-defined polymers by several controlled polymerization techniques that have developed over the decades [7–9].

Nowadays, it is easy to prepare polypeptides by adjusting the feed ratio and reaction conditions, culminating in anti-bacterial activity [9, 10]. Moreover, the synthetic polypeptides were less prone to proteolytic attack as compared to natural anti-bacterial peptides. The careful design and synthesis of these anti-bacterial polypeptides allowed for the customization of their properties, enabling them to target specific pathogens effectively. By understanding the mechanisms of action for natural anti-bacterial peptides, researchers can optimize the structure and composition of synthetic polypeptides to enhance their antimicrobial activity. This innovative strategy not only harnesses nature's defense mechanisms but also offers the potential for the development of new antimicrobial materials with diverse applications [10–12]. Several studies have reported that star-shaped polypeptides exhibited excellent anti-bacterial activity due to their unique topological structures [10, 13]. The star-shaped polypeptides could interact with bacterial cell membranes and result in the disruption of bacterial morphology and subsequent cell death. These studies have demonstrated that the arm number and peptide chain length could affect biocompatibility and antimicrobial activity. Moreover, the grafting of hydrophobic groups onto star-shaped PLL was found to improve their cytotoxic selectivity toward pathogens over mammalian cells [14]. Previous studies also demonstrated that cationic, $\alpha$-helical polypeptides exhibited anti-bacterial activity against both gram-positive and gram-negative bacteria by interacting with bacterial cell membrane [15, 16]. Therefore, designing and synthesizing anti-bacterial polypeptide not only provides a more sustainable alternative to traditional antimicrobial agents but also addresses the growing concern of anti-bacterial resistance.

To augment biocompatibility and anti-bacterial activity, it is common practice to graft natural small molecules onto the side chains of polypeptides [14, 17]. Several studies have demonstrated that anti-bacterial polypeptides composed of hydrophobic groups could improve their interactions with lipid membranes via hydrophobic interactions [18, 19]. Herein, we aim to study the effect of polypeptide composition on the biocompatibility and bioactivity against bacteria. The positively charged PLL is a well-known anti-bacterial polypeptide [17, 20]. Three hydrophobic peptide segments, poly(L-alanine) ($Ala_n$), poly(L-leucine) ($Leu_n$) and poly(L-phenylalanine) ($Phe_n$), were selected to tether with PLL segment to form block copolypeptides. Linear and 3-armed block copolypeptides were prepared and examined their biocompatibility as well as anti-bacterial activity. In addition to understand the anti-bacterial activity of block copolypeptides against *Staphylococcus aureus* (*S. aureus*) and *Shigella flexneri* (*S. flexneri*) in vitro, *Caenorhabditis elegans* (*C. elegans*) was used as an in vivo infected model to assess the potential of the polypeptides to protect nematodes from bacterial infection. It is anticipated that the tethering of hydrophobic peptide segments onto PLL would be able to improve not only their biocompatibility but also their anti-bacterial activity. With the versatility of the ring-opening polymerization, these anti-bacterial polypeptides could be introduced in the hydrogels or on the substrates to endow them with anti-bacterial functions.

## Materials and methods

### Materials

All the reagents were in ACS grade. 1-Hexylamine and tris(2-aminoethyl)amine were purchased from Sigma-Aldrich. Calcium hydride (95%), sodium cubes (99.95% in mineral oil), L-alanine, L-leucine and L-phenylalanine were supplied by Sigma-Aldrich. Hexane and diethyl ether were purchased from ECHO. Tetrahydrofuran (THF) was purchased from J.T. Baker. Trifluoroacetic acid (TFA, 99%) was purchased from Alfa Aesar, hydrogen bromide solution (33 wt% HBr in acetic acid) was purchased from Acros. Trifluoroacetic acid-$d_1$ (99.5%, Sigma-Aldrich), $D_2O$ (99.9%, Sigma-Aldrich), triphosgene (98%, Sigma-Aldrich), Z-L-lysine (99%, Sigma-Aldrich) and Tris(2-aminoethyl)amine (Tren, 98%, Sigma-Aldrich).

### Synthesis and deprotection of linear and star-shaped polypeptides

Linear and 3-armed block copolypeptides were synthesized by ring-opening polymerization (ROP) of *N*-carboxyanhydrides (NCAs) according to the procedures reported in the previous reports [21–23]. Firstly, NCAs of Z-L-lysine (ZLL), L-alanine (Ala), L-leucine (Leu) and L-phenylalanine (Phe) were synthesized by reacting with triphosgene in THF at 55 °C under argon atmosphere, followed by recrystallization using n-hexane [20–23]. For the synthesis of linear block copolypeptides, 1-hexylamine was used as the initiator and the molar ratio of the initiator, ZLL NCAs and other NCAs was set to be 1: 20: 10 [24, 25]. After adding a designated amount of the solution to the ZLL NCA solution, the reaction mixture was stirred at room temperature for 72 h under argon atmosphere. After 72 h, the designated amount of other NCAs such as Ala, Leu or Phe NCAs in anhydrous THF was added to the reaction mixture and stirred at room temperature for an additional 72 h. For synthesis of 3-armed block copolypeptides, tris(2-aminoethyl)amine (Tren) was used as the initiator and the molar ratio of the initiator to the two NCAs was set to be 1: 30: 15. The detailed synthesis procedures were shown in the previously reported literatures [14, 26]. The Tren initiator and ZLL NCA solutions in anhydrous THF were prepared in a glove box. After adding a designated amount of the initiator solution to the ZLL NCA solution, the reaction mixture was stirred at room temperature for 72 h under argon atmosphere. After 72 h, the designated amount of other NCA solutions in anhydrous THF was added to the reaction mixture and stirred at room temperature for an additional 72 h. Finally, the as-synthesized polypeptides were purified by precipitating in anhydrous diethyl ether. All the block copolypeptides, which were $Lys_{20}$-$Ala_{10}$, $Lys_{20}$-$Leu_{10}$, $Lys_{20}$-$Phe_{10}$, 3s-$Lys_{10}$-$Ala_5$, 3s-$Lys_{10}$-$Leu_5$ and 3s-$Lys_{10}$-$Phe_5$, were obtained by removing the protecting Z group on PZLL segment using hydrogen bromide (HBr, 33 wt% in acetic acid, Sigma-Aldrich) in trifluoroacetic acid (TFA, Sigma-Aldrich) for 30 min, followed by precipitation using ethyl ether (> 99%, ECHO) and lyophilization after dialysis against DI water. The typical yields for the linear and 3-armed block copolypeptides were between 80 and 90%.

### Characterization of polypeptides

The polypeptides were characterized by nuclear magnetic resonance (NMR) and gel permeation chromatograph-light scattering (GPC-LS) analyses to derive degree of polymerization (DP), block ratio, number-average molecular weights ($M_n$) and molecular weight distribution ($M_w/M_n$). For the NMR analysis, the polypeptides containing Z group were dissolved in trifluoroacetic acid-d (TFA-*d*), and the polypeptides after deprotection of Z group were dissolved in deuterium oxide ($D_2O$). Based on the $^1$H NMR spectra, the integral areas of the protons on the initiators and two peptide segments were used to calculate the DPs and block ratios of all the block copolypeptides. Other protons on the two peptide segments were also used to check their block ratios and the consistent values were obtained and labeled as subscript in the sample names. The $M_n$ and $M_w/M_n$ of the PZLL polypeptides were characterized by GPC-LS analysis. The samples were dissolved in DMF and filtrated with 0.22 μm PTFE filter (13 mm, Finetech). The GPC-LS system equipped with three Viscotek detectors and two Shodex GPC columns was operated at 55 °C and 0.8 mL min$^{-1}$ of flow rate. The eluent solution was DMF containing 0.1 M LiBr and polystyrene (molecular weight: 25,000 g mol$^{-1}$) was used as the calculation standard. The polypeptide chain conformations were characterized by Fourier transform infrared (FTIR, Thermo Nicolet Nexus 6700 FTIR spectrometer) and circular dichroism (CD, AVIV Model 410 spectrometer) analyses. Attenuated total reflectance Fourier transform infrared (ATR-FTIR) spectra of polypeptide samples were measured with a Thermo Nicolet Nexus 670 FTIR. CD spectra of polypeptide samples were measured at the concentration of 0.1 mg mL$^{-1}$ in DI water on a JASCO J-815 spectrometer (JASCO, Japan) from 190 to 260 nm of the wavelength. The percentages of secondary conformations adopted by peptides were computed by fitting the CD spectra using the *BeStSel* software.

### Hemolysis assay

The hemolytic activity of polypeptides was assessed based on the following procedures. Human red blood cells (hRBCs) were centrifuged to obtain the pallet, followed by washing with phosphate buffered saline (PBS; pH 7.0, 0.15 N). Upon repeating the washing process three times, the hRBCs were suspended in PBS with 10 vol%. The polypeptide solution (100 μL) was incubated with equal volume of hRBCs (10 vol%) in sterile 96-well plates for 1 h at 37 °C. Positive and negative controls were established using 0.1 vol% Triton X-100 and 0.1 M PBS, respectively. After incubation, the mixtures were centrifuged at 2500 rpm for 3 min, transferred to fresh 96-well plates, and measured the absorbance intensity of the supernatant at 405 nm by the micro plate reader (Epoch Gen 5). The percentage of hemolysis was calculated by the following formula:

$$\text{Hemolysis}(\%) = \left(\text{Abs}_{\text{Polypeptide solution}} - \text{Abs}_{\text{PBS}}\right) / \left(\text{Abs}_{\text{TritonX}-100(0.1\%)} - \text{Abs}_{\text{PBS}}\right) \times 100\%$$

### Organoid cytotoxicity test

NIH/3T3 and BEAS-2B cells were cultured in the round bottom 96-well plate ($2 \times 10^4$ cells/well). After 24 h incubation with polypeptides, the organoid viability was evaluated using the WST-8 reagent. Serum-free cell-medium-contained WST-8 reagent was added to the organoid and incubated at 37 °C for 1 h. The resulting solution was measured at a wavelength of 450 nm using the microplate reader (Epoch Gen 5), according to the absorbance intensity at 450 nm to calculate the cytotoxicity of cellular organoid.

Cell viability was transformed from absorbance by the following formula:

$$\text{Cell viability}(\%) = \left(\text{OD}_{\text{sample}} - \text{OD}_{\text{blank}}\right) / \left(\text{OD}_{\text{normal}} - \text{OD}_{\text{blank}}\right) \times 100\%$$

In the formula, $\text{OD}_{\text{sample}}$, $\text{OD}_{\text{blank}}$ and $\text{OD}_{\text{normal}}$ represented the absorbance of WST-8 reagent. Subscript (sample) represented cells treated with polypeptide in the well. Subscript (blank) represented wells with only cell culture medium containing WST-8 reagent. Subscript (normal) represented cells without any treatment in the well.

### In vitro *anti-bacterial activity test*

*Shigella flexneri* (*S. flexneri*) and *Staphylococcus aureus* (*S. aureus*) bacteria were provided by the Bioresource Collection and Research Center (Hsinchu, Taiwan). The half maximal inhibitory concentration ($IC_{50}$) and minimal inhibitory concentration (MIC) were determined by contact method. Briefly, 900 μL of a bacterial suspension at $1 \times 10^5$ CFU were cocultured with 100 μL of the polypeptide solution in 1.5 mL eppendorf. Then, this mixture was placed in a 37 °C incubator with a rotation speed of 150 rpm and cocultured for 1 h. After cocultivation, 10 μL of sample was inoculated onto LB agar plate. After 18 h, colony on LB agar plate was calculated with followed formula:

$$\text{Viability}\ (\%) = N_t / N_c \times 100\%$$

where $N_c$ and $N_t$ represented the number of colonies on the agar plate after 24 h of incubation at 37 °C. Subscript (*c*) and (*t*) represented bacteria without any treatment and treated with polypeptide in the 1.5 mL eppendorf, respectively.

The morphology of bacteria after treatment with polypeptide at 37 °C for 24 h was imaged using field emission scanning electron microscopy (FE-SEM) analyses were carried out on Hitachi SU8010. The samples were fixed by a glutaraldehyde solution (1%) at 4 °C for 1.5 h. Then, the samples were dehydrated through a series of ethanol solutions (30%, 50%, 70%, 80%, 90% and 100%) at room temperature. After dehydration, the samples were treated with tert-butyl alcohol at 4 °C and lyophilized for 12 h.

The growth kinetics of bacteria after treatment with polypeptide was identified by examining the absorbance at the wavelength of 600 nm. At 0, 2, 4, 6, 8, 10, 12, 20

and 24 h, the experimental group consists of 1.4 mL of LB solution, 0.4 mL of the respective polypeptide at its $IC_{50}$ concentration and 0.2 mL of pre-quantified bacterial suspension at $1 \times 10^6$ CFU for time-kill kinetics assay. The blank group consists of 1.4 mL of LB solution, 0.4 mL of the sample solution and 0.2 mL of sterile water. All groups are placed in a 37 °C incubator at a rotation speed of 150 rpm for coculturing.

#### In vivo *anti-bacterial activity test*

*C. elegans* was used as in vivo infection model. Nematodes were cultured on the bacterial lawn from *S. aureus* and *S. flexneri* ($1 \times 10^5$ CFU) which has preincubated with polypeptide. For the preparation of bacterial lawn, bacteria were co-incubated with polypeptide solution at their MIC for 1 h at 37 °C and then spread onto 6 cm nematode growth (NG) agar plate. *C. elegans* at the synchronized L4 stage were placed on these plates and were incubated at 20 °C. To ensure the well-being of the population, the nematodes were daily moved to new plates. A daily inspection was performed using the dissecting microscope, with any nematodes displaying a lack of pharyngeal pumping considered as deceased. Nematodes that had left the plates were excluded from the study.

#### Statistical analysis

The data were reported as the Mean ± SEM. The differences of survival curve between different groups were analyzed by Mantel–Cox log-rank test. Statistical significance was set to $*p < 0.05$, $**p < 0.01$ and $***p < 0.001$.

## Results and discussions

#### Synthesis and characterization of polypeptides

The Z-protected block copolypeptides were synthesized according to the synthesis procedures and the block copolypeptides ($Lys_{20}$-$Ala_{10}$, $Lys_{20}$-$Leu_{10}$, $Lys_{20}$-$Phe_{10}$, 3s-$Lys_{10}$-$Ala_5$, 3s-$Lys_{10}$-$Leu_5$ and 3s-$Lys_{10}$-$Phe_5$) were obtained by the deprodection of Z group using HBr (Scheme 1). GPC-LS and $^1$H NMR analyses were used to determine their DPs and block ratios. As shown in Figs. S1 and S2, all the protons in the $^1$H NMR spectra could be assigned to those on the block copolypeptides, suggesting the successful synthesis of these Z-protected block copolypeptides. The integral areas of the protons on the initiators and peptide segments were used to calculate the DPs and block ratios of these Z-protected block copolypeptides. For example, based on the $^1$H NMR spectra of ZLys$_{20}$-Phe$_{10}$ and 3s-ZLys$_{10}$-Phe$_5$ (Figs. S1 and S2), the integral areas of the protons on the initiators ($CH_3CH_2$– or –$NCH_2$–), the ε protons on PZLL (or –$(CH_2)_3CH_2$–) and the protons of benzyl group on the peptide chain (–$COOCH_2C_6H_5$ and –$CH_2C_6H_5$) were used to calculate the DPs and block ratios as summarized in Table S2. For other Z-protected block copolypeptides, the

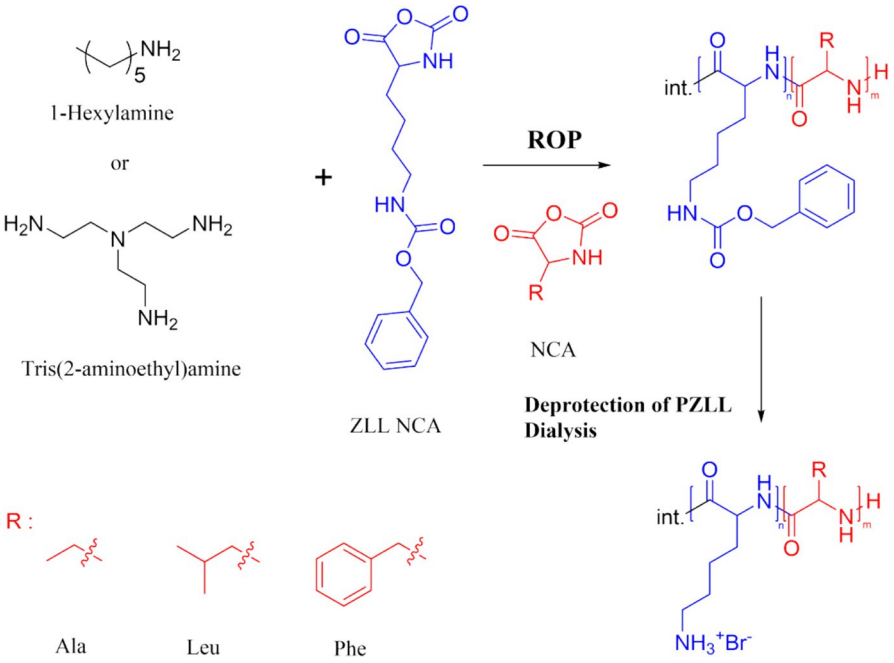


**Scheme 1** Synthesis scheme of the linear and 3-armed block copolypeptides

protons on the peptide chain were used to calculate the DPs and block ratios. The calculated DP and block ratio values for the two peptide segments were comparable with the feed molar ratios (Table S1). Upon preparing the 3-armed PZLL first block, a small portion of the reaction solution was drawn and purified for GPC-LS analysis, and the DPs of the 3-armed PZLL segment derived from the GPC-LS analysis were comparable with those derived from the NMR analysis (data not shown). Upon deprotection, the integral areas of the protons of benzyl group on the PZLL segments significantly decreased (Figs. S3 and S4), suggesting the successful removal of the Z group.

The chain conformations of block copolypeptides were elucidated by FTIR and CD analyses at neutral condition (Fig. 1). The FTIR spectra of polypeptides indicated specific peaks which were associated with different secondary conformation. All the as-synthesized polypeptides exhibited the amide I absorption peak at approximately 1650 $cm^{-1}$ (Fig. 1a and b), indicating signals associated with both random coil and $\alpha$-helical conformations. The amide I absorption peaks at around 1625 and 1675 $cm^{-1}$ were the indicative of signals associated with $\beta$-sheet and $\beta$-turn conformations, respectively. A broad absorption peak between 1500 and 1550 $cm^{-1}$ was identified as a signal related to amide II. The CD spectra showed that all the polypeptides exhibited negative peaks in the wavelength range of 190–200 nm (Fig. 1c and d), which could be attributed to the presence of random coil conformation within PLL. It is well-known that the PLL segment would adopt mainly random coil conformation at neutral condition [27, 28]. Additionally, it was

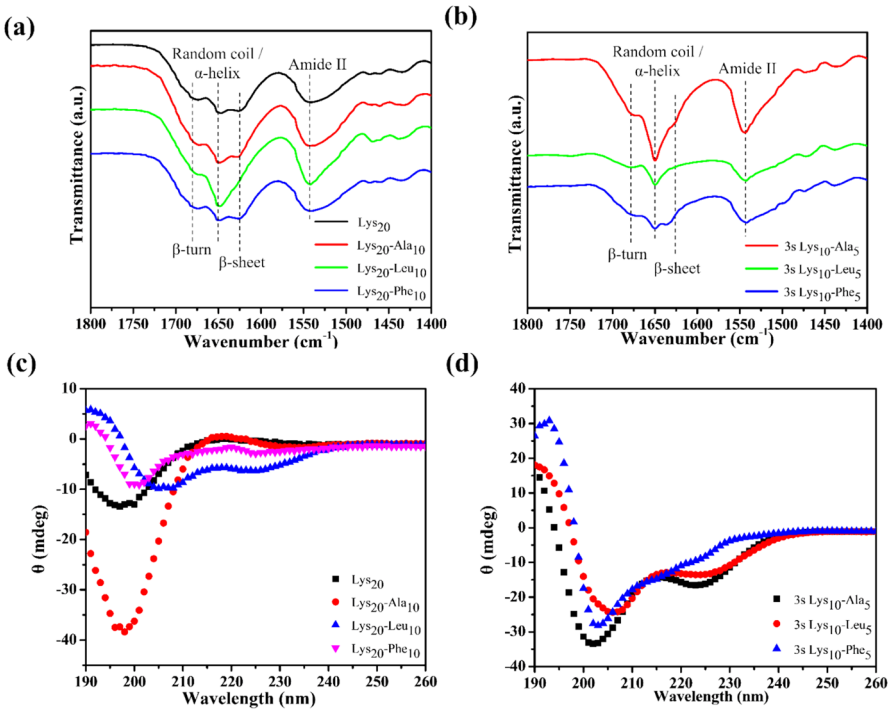


**Fig. 1** Secondary conformation of polypeptides. **a**, **b** FTIR and **c**, **d** CD spectra of linear and 3-armed block copolypeptides. The polypeptide concentration of 0.1 mg $mL^{-1}$ in DI water was used for CD analysis

observed that both linear and 3-armed block copolypeptides containing Leu moieties exhibited prominent peaks at 208 and 222 nm, which could be attributed to the presence of $\alpha$-helical conformation within $Leu_n$ peptide segment. The percentages of different secondary conformations adopted by the block copolypeptides are presented in Table 1. It was obvious that the random coil and ordered ($\alpha$-helix and/or $\beta$-sheet/ $\beta$-turn) conformations were originated from the PLL and hydrophobic peptide segments, respectively. Previous studies have demonstrated that the PLL

**Table 1** The percentages of different secondary conformations adopted by the block copolypeptides computed by using the *BeStSel* software

| Polypeptides | Random coil (%) | $\alpha$-helix (%) | $\beta$-sheet/ $\beta$-turn (%) |
|---|---|---|---|
| $Lys_{20}$ | 48.8 | 0 | 27.9/23.3 |
| $Lys_{20}$-$Ala_{10}$ | 50.6 | 0 | 27.5/21.9 |
| $Lys_{20}$-$Leu_{10}$ | 49.8 | 26.5 | 12.5/11.1 |
| $Lys_{20}$-$Phe_{10}$ | 55.5 | 3.0 | 23.2/18.3 |
| 3s-$Lys_{10}$-$Ala_5$ | 51.6 | 19.8 | 18.6/10.0 |
| 3s-$Lys_{10}$-$Leu_5$ | 43.7 | 29.4 | 12.7/14.2 |
| 3s-$Lys_{10}$-$Phe_5$ | 64.3 | 12.6 | 13.1/9.9 |

tethered with a hydrophobic peptide chain on the chain end or grafted a hydrophobic group on the side chain could facilitate the PLL adopting more ordered conformation due to the confinement of PLL chains [27, 28]. It is known that the long $Leu_n$ ($n > 20$) peptide segment mainly adopted $\alpha$-helical conformation, whereas the $Phe_n$ peptide segment ($n = 10$–$20$) mainly adopted a $\beta$-sheet/ $\beta$-turn conformation [29, 30]. One previous study has shown that the $\alpha$PEG-$Ala_{12}$ adopted a $\alpha$-helical conformation at the concentration below 0.05 mg $mL^{-1}$ in DI water and then a helix-to-sheet conformational transition occurred upon the increase in the concentration above 0.1 mg $mL^{-1}$, which could be attributed to the interchain hydrogen bonding interactions [31]. For $Lys_{20}$-$Leu_{10}$ and 3s-$Lys_{10}$-$Leu_5$ polypetpipdes, the short $Leu_n$ peptide segments adopted a mixture of $\alpha$-helical and $\beta$-sheet/ $\beta$-turn conformations. The linear $Lys_{20}$-$Ala_{10}$ and $Lys_{20}$-$Phe_{10}$ mainly adopted a mixture of random coil and $\beta$-sheet/ $\beta$-turn conformations, suggesting that the $Ala_{10}$ and $Phe_{10}$ peptide segments mainly adopted a $\beta$-sheet/ $\beta$-turn conformation due to the interchain hydrogen bonding interactions. Rather, 3s-$Lys_{10}$-$Ala_5$ and 3s-$Lys_{10}$-$Phe_5$ exhibited a mixture of random coil, $\alpha$-helical, and $\beta$-sheet/ $\beta$-turn conformations. The presence of $\alpha$-helical conformation with a low percentage might originate from the confinement of PLL segment.

### In vitro *biocompatibility of polypeptides*

To understand the biocompatibility of these polypeptides, the hemolysis and cell organoid cytotoxicity tests were conducted to evaluate to their cytotoxicity (Figs. 2 and S5). Previous studies have demonstrated that the hemolytic activity of $Lys_{20}$ against RBCs was lower than 5% [14]. In this study, $Lys_{20}$, $Lys_{20}$-$Ala_{10}$ and 3s-$Lys_{10}$-$Ala_5$ were found to exhibit low hemolytic activity, whereas other block polypeptides, which were those tethered with $Leu_n$ and $Phe_n$ peptide segments, showed significantly higher hemolytic activity upon the increase in polypeptide concentration (Fig. 2a). The results showed that the tethered $Ala_n$ peptide segment would not result in the increase in the hemolytic activity of the as-synthesized polypeptides. The cell viability tests of NIH/3T3 and BEAS-2B cell spheres after treatment of $Lys_{20}$, $Lys_{20}$-$Ala_{10}$ and 3s-$Lys_{10}$-$Ala_5$ were further assessed. The cell viability of NIH/3T3

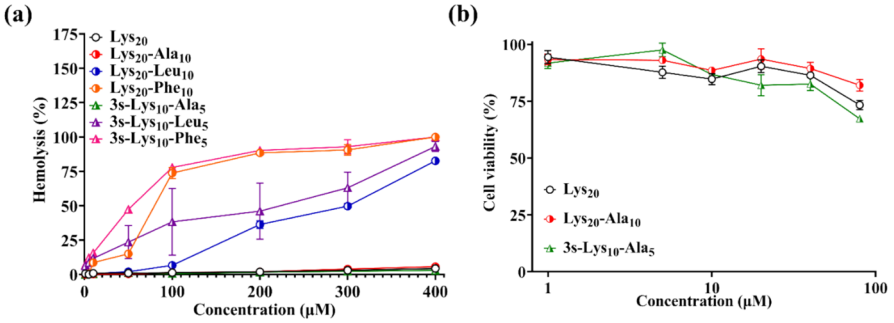


**Fig. 2** The biocompatibility of block copolypeptides. **a** Hemolytic activity and **b** cell viability of NIH/3T3 cell organoids after treatment with polypeptides (n = 3)

cell organoids was higher than 80% as the organoids treated with the polypeptides at concentrations lower than 40 μM (Fig. 2b). The cell viability of BEAS-2B cell organoids was over 80% as the organoids treated with the polypeptides at concentrations lower than 20 μM (Fig. S5). The screening results demonstrated that $Lys_{20}$, $Lys_{20}$-$Ala_{10}$ and 3s-$Lys_{10}$-$Ala_5$ were biocompatible.

### In vitro anti-bacterial activity of polypeptides against *S. aureus* and S. flexneri

The above results showed that $Lys_{20}$, $Lys_{20}$-$Ala_{10}$ and 3s-$Lys_{10}$-$Ala_5$ were biocompatible, and these polypeptides were selected for assessing their anti-bacterial activities. The viability, growth curve and morphology of *S. aureus* and *S. flexneri* after treatment with polypeptides were analyzed (Fig. 3). It was obvious that these polypeptides exhibited anti-bacterial activities against *S. aureus* and *S. flexneri* as the concentration of polypeptides was at 40 μM (Fig. 3a and c). The viability of *S. aureus* and *S. flexneri* after treatment exhibited a dose dependent manner. The MIC and MBC of *S. aureus* and *S. flexneri* after treatment were determined and summarized in Table 2. 3s-$Lys_{10}$-$Ala_5$ exhibited the best anti-bacterial activity

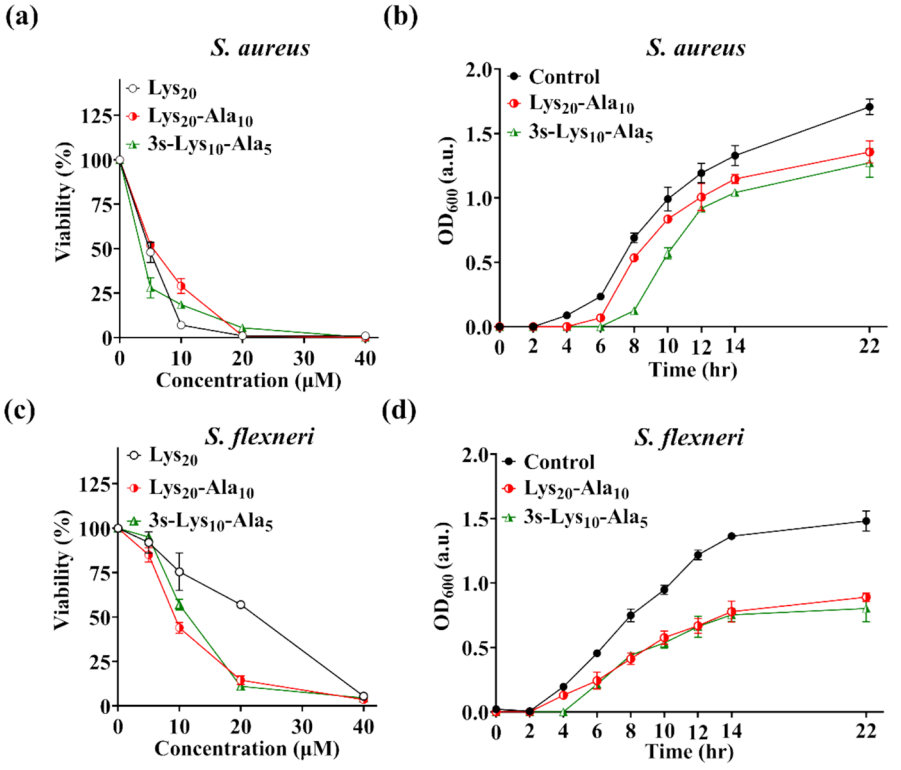


**Fig. 3** The anti-bacterial activities of block copolypeptides. **a**, **c** viability and **b**, **d** growth curves after treatment of block copolypeptides (n = 3)

**Table 2** MIC and MBC of *S. aureus* and *S. flexneri* after treatment of linear $Lys_{20}$, $Lys_{20}$-$Ala_{10}$ and 3s-$Lys_{10}$-$Ala_5$ block copolypeptides

| Sample code | *S. aureus* | | *S. flexneri* | |
|---|---|---|---|---|
| | MIC (μM) | MBC (μM) | MIC (μM) | MBC (μM) |
| $Lys_{20}$ | 10.2 | 40 | 38.3 | 40 |
| $Lys_{20}$-$Ala_{10}$ | 14.9 | 40 | 21.0 | 40 |
| 3s-$Lys_{10}$-$Ala_5$ | 9.7 | 40 | 19.8 | 40 |

against *S. aureus* among all, whereas both $Lys_{20}$-$Ala_{10}$ and 3s-$Lys_{10}$-$Ala_5$ exhibited comparable anti-bacterial activities against *S. flexneri*, which was much better than $Lys_{20}$. The bacterial growth inhibited by the polypeptides was evaluated by measuring the $OD_{600}$ at different time periods (Fig. 3b and d). The $OD_{600}$ values for the control groups of both *S. aureus* and *S. flexneri* were achieved to 0.75, and the slope of bacterial growth curve was significant change at 8 h, suggesting that both bacteria into log phase at this time point. In contrast, the reduction of the $OD_{600}$ values for the groups treated with polypeptides, supporting that polypeptide exhibited inhibitory effects to bacteria, consistent with the results of the bacterial viability after treatment. Previous studies have demonstrated that star-shaped polypeptide exhibited higher antimicrobial ability than the linear counterparts via multifaceted interactions with bacterial cell membrane [13, 14]. In this study, the multifaceted interactions between 3s-$Lys_{10}$-$Ala_5$ and *S. aureus* bacterial cell membrane might be significant, leading to the best anti-bacterial activity of 3s-$Lys_{10}$-$Ala_5$ against *S. aureus* among all. However, the multifaceted interactions between 3s-$Lys_{10}$-$Ala_5$ and *S. flexneri* bacterial cell membrane might not be pronounced, leading to both $Lys_{20}$-$Ala_{10}$ and 3s-$Lys_{10}$-$Ala_5$ exhibited comparable anti-bacterial activities against *S. flexneri*.

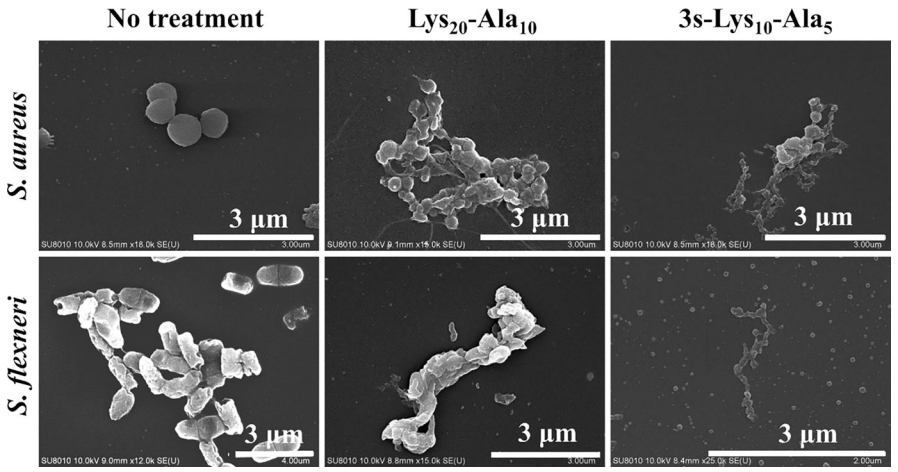


**Fig. 4** FE-SEM images of bacterial morphology of *S. aureus* and *S. flexneri* with no treatment and after treatment of block copolypeptides

The morphology of bacteria after treatment with $Lys_{20}$-$Ala_{10}$ and 3s-$Lys_{10}$-$Ala_5$ polypeptides was further investigated by FE-SEM analysis (Fig. 4). With no treatment, the cell membranes of *S. aureus* and *S. flexneri* were intact without rupture. On the contrary, the cell membranes of *S. aureus* and *S. flexneri* were disrupted after incubation with polypeptides at the $IC_{50}$ concentration. Moreover, the FE-SEM images showed that the extent of rupture was more significant in the group treated with 3s-$Lys_{10}$-$Ala_5$ polypeptide. Thus, these findings demonstrated that the polypeptides displayed potent antimicrobial effects by disrupting the integrity of bacterial cell membranes, ultimately leading to bacterial rupture. The anti-bacterial mechanism of the polypeptides possibly involved processes associated to adhesion and destruction. That is, the polypeptides might adhere to cell membrane through electrostatic interactions between positively charged PLL segment and negatively charged membrane and the insertion of $Ala_n$ segment into the membrane bilayer via hydrophobic interactions.

### In vivo infection model of *C. elegans* survival rate

To understand whether $Lys_{20}$-$Ala_{10}$ and 3s-$Lys_{10}$-$Ala_5$ block copolypeptides inhibit *S. aureus* and *S. flexneri* in vivo, *C. elegans* was used as the in vivo infection model, which has been commonly used for studying human infectious diseases by bacterial infections [32, 33]. The worms were fed on bacteria pretreated with polypeptides at the MIC concentrations. The Mantel–Cox log-rank tests verified that the nematodes fed with polypeptide-pretreated bacteria showed prolonged lifespan as compared to the control group (Fig. 5), revealing that peptide-pretreated bacteria have a protective effect on nematodes. It could be observed that the median lifespan of the group treated with 3s-$Lys_{10}Ala_5$ polypeptide was longer than that of the group treated with $Lys_{20}$-$Ala_{10}$ one, suggesting that 3s-$Lys_{10}$-$Ala_5$ polypeptide exhibited better treatment than $Lys_{20}$-$Ala_{10}$ one.

## Conclusions

This study investigated the biocompatibility and anti-bacterial activity against *S. aureus* and *S. flexneri* of linear and 3-armed block copolypeptides including $Lys_{20}$-$Ala_{10}$, $Lys_{20}$-$Leu_{10}$, $Lys_{20}$-$Phe_{10}$, 3s-$Lys_{10}$-$Ala_5$, 3s-$Lys_{10}$-$Leu_5$ and 3s-$Lys_{10}$-$Phe_5$. $Lys_{20}$-$Ala_{10}$ and 3s-$Lys_{10}$-$Ala_5$ block copolypeptides exhibited excellent biocompatibility and potent anti-bacterial activity, while the others exhibited potent anti-bacterial activity rather exhibiting cell toxicity. The results revealed that the tethering of hydrophobic $Ala_n$ segments onto PLL improved not only their biocompatibility but also their anti-bacterial activity. These polypeptides exhibited potent anti-bacterial activity against *S. aureus* and *S. flexneri*, as evidenced in our in vitro experiments. The in vitro results were further validated in an in vivo infection model using *C. elegans*, showing an extended lifespan in *C. elegans* after treatment with polypeptide-pretreated bacteria. These collective findings, both from in vitro and in vivo models, led us to propose the potential use of

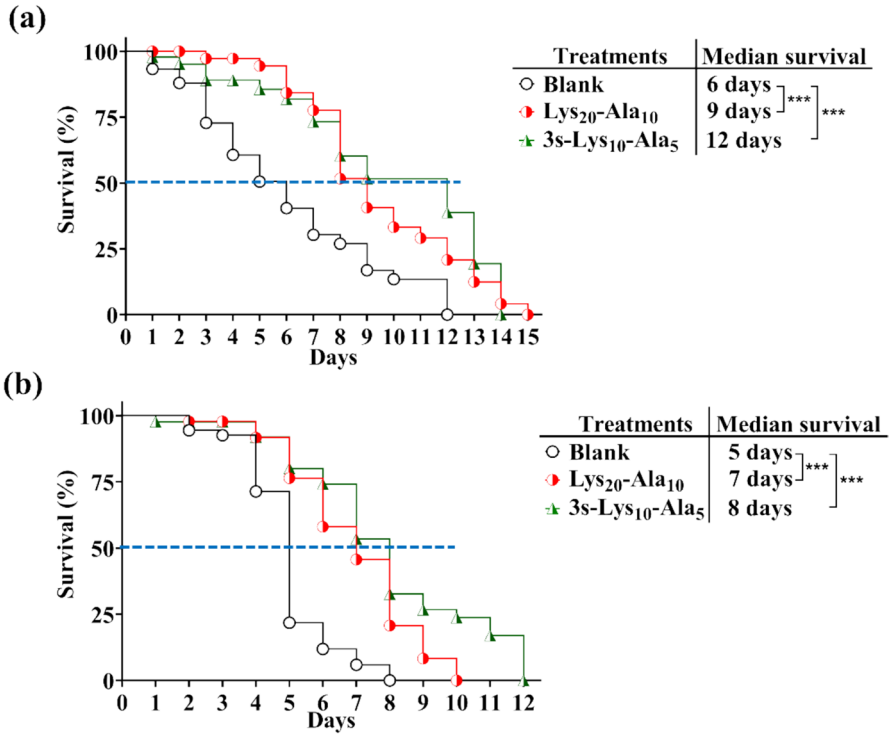


**Fig. 5** Survival curves of lifespan in *C. elegans* fed on **a** *S. aureus* and **b** *S. flexneri* treatment with $Lys_{20}$-$Ala_{10}$ and 3s-$Lys_{10}$-$Ala_5$ block copolypeptides

$Lys_{20}$-$Ala_{10}$ and 3s-$Lys_{10}$-$Ala_5$ as candidates for the development of treatments against bacterial infections caused by *S. aureus* and *S. flexneri*. This suggested a promising new avenue of research for the development of novel anti-bacterial agents, which would be promising in the biomedical field.

**Supplementary Information** The online version contains supplementary material available at https://doi.org/10.1007/s00289-024-05574-6.

**Acknowledgements** The authors acknowledge the financial support from the National Science and Technology Council, Taiwan (NSTC 110-2221-E-006-002-MY3 and 112-2221-E-006-011-MY3). The authors are grateful for the support from the use of code of the machine equipment belonging to the Core Facility Center of National Cheng Kung University. We thank Bi-Yun Lin (Instrument Center, National Cheng Kung University) for the help in performing the NMR experiments. We thank Professor Chang-Shi Chen provided *C. elegans*.

**Author contributions** Ying-Jung Cheng performed conceptualization, formal analysis, investigation and writing—original draft. Yi-Sheng Jiang presented data curation, validation, investigation and writing—original draft. Cheng-Rung Huang provided formal analysis, validation, visualization, methodology and resources. Chang-Shi Chen carried out methodology and resources. Jeng-Shiung Jan conducted conceptualization, supervision, funding acquisition, project administration and writing—review & editing.

**Data availability** The data that support the findings of this study are available from the corresponding author upon reasonable request.

## Declarations

**Conflicts of interest** The authors declare no competing interests.

## References


1. Maurya D, Nisal R, Ghosh R, Kambale P, Malhotra M, Jayakannan M (2023) Fluorophore-tagged poly(L-Lysine) block copolymer nano-assemblies for real-time visualization and antimicrobial activity. Eur Polym J 183:111754. https://doi.org/10.1016/j.eurpolymj.2022.111754
2. Masters EA, Trombetta RP, de Mesy Bentley KL, Boyce BF, Gill AL, Gill SR, Nishitani K, Ishikawa M, Morita Y, Ito H, Bello-Irizarry SN, Ninomiya M, Brodell JD, Lee CC, Hao SP, Oh I, Xie C, Awad HA, Daiss JL, Owen JR, Kates SL, Schwarz EM, Muthukrishnan G (2019) Evolving concepts in bone infection: redefining "biofilm", "acute vs. chronic osteomyelitis", "the immune proteome" and "local antibiotic therapy." Bone Res. https://doi.org/10.1038/s41413-019-0061-z
3. Godoy-Gallardo M, Eckhard U, Delgado LM, de Roo Puente YJD, Hoyos-Nogués M, Gil FJ, Perez RA (2021) Antibacterial approaches in tissue engineering using metal ions and nanoparticles: from mechanisms to applications. Bioact Mater 6:4470–4490. https://doi.org/10.1016/j.bioactmat.2021.04.033
4. Xuan J, Feng W, Wang J, Wang R, Zhang B, Bo L, Chen Z-S, Yang H, Sun L (2023) Antimicrobial peptides for combating drug-resistant bacterial infections. Drug Resist 68:100954. https://doi.org/10.1016/j.drup.2023.100954
5. Mahlapuu M, Björn C, Ekblom J (2020) Antimicrobial peptides as therapeutic agents: opportunities and challenges. Crit Rev Biotechnol 40:978–992. https://doi.org/10.1080/07388551.2020.1796576
6. Levin A, Hakala TA, Schnaider L, Bernardes GJ, Gazit E, Knowles TP (2020) Biomimetic peptide self-assembly for functional materials. Nat Rev Chem 4:615–634. https://doi.org/10.1038/s41570-020-0215-y
7. Shabani S, Hadjigol S, Li W, Si Z, Pranantyo D, Chan-Park MB, O'Brien-Simpson NM, Qiao GG (2024) Synthetic peptide branched polymers for antibacterial and biomedical applications. Nat Rev Bioeng 2:343–361. https://doi.org/10.1038/s44222-023-00143-4
8. Zhu M-M, Fang Y, Chen Y-C, Lei Y-Q, Fang L-F, Zhu B-K, Matsuyama H (2021) Antifouling and antibacterial behavior of membranes containing quaternary ammonium and zwitterionic polymers. J Colloid Interface Sci 584:225–235. https://doi.org/10.1016/j.jcis.2020.09.041
9. Gan BH, Gaynord J, Rowe SM, Deingruber T, Spring DR (2021) The multifaceted nature of antimicrobial peptides: current synthetic chemistry approaches and future directions. Chem Soc Rev 50:7820–7880. https://doi.org/10.1039/D0CS00729C
10. Shabani S, Hadjigol S, Li W, Si Z, Pranantyo D, Chan-Park MB, O'Brien-Simpson NM, Qiao GG (2024) Synthetic peptide branched polymers for antibacterial and biomedical applications. Nat Rev Bioeng 2:343–361. https://doi.org/10.1038/s44222-023-00143-4
11. Munoz-Bonilla A, Fernandez-Garcia M, Rodriguez-Hernandez J (2014) Towards hierarchically ordered functional porous polymeric surfaces prepared by the breath figures approach. Prog Polym Sci 39:510–554. https://doi.org/10.1016/j.progpolymsci.2013.08.006
12. Jiang Y, Chen Y, Song Z, Tan Z, Cheng J (2021) Recent advances in design of antimicrobial peptides and polypeptides toward clinical translation. Adv Drug Deliv Rev 170:261–280. https://doi.org/10.1016/j.addr.2020.12.016
13. Laroque S, Garcia Maset R, Hapeshi A, Burgevin F, Locock KES, Perrier S (2023) Synthetic star nanoengineered antimicrobial polymers as antibiofilm agents: bacterial membrane disruption and cell aggregation. Biomacromol 24:3073–3085. https://doi.org/10.1021/acs.biomac.3c00150
14. Chen Y-F, Lai Y-D, Chang Y-H, Tsai Y-C, Tang C-C, Jan J-S (2019) Star-shaped polypeptides exhibit potent antibacterial activities. Nanoscale 11:11696–11708. https://doi.org/10.1039/C9NR02012H
15. Xiong M, Bao Y, Xu X, Wang H, Han Z, Wang Z, Liu Y, Huang S, Song Z, Chen J, Peek RM Jr, Yin L, Chen L-F, Cheng J (2017) Selective killing of Helicobacter pylori with pH-responsive helix-coil conformation transitionable antimicrobial polypeptides. Proc Natl Acad Sci USA 114:12675–12680. https://doi.org/10.1073/pnas.1710408114

16. Xiong M, Lee MW, Mansbach RA, Song Z, Bao Y, Peek RM Jr, Yao C, Chen LF, Ferguson AL, Wong GC, Cheng J (2015) Helical antimicrobial polypeptides with radial amphiphilicity. Proc Natl Acad Sci USA 112:13155–13160. https://doi.org/10.1073/pnas.1507893112
17. Hsu FM, Hu MH, Jiang YS, Lin BY, Hu J-J, Jan J-S (2020) Antibacterial polypeptide/heparin composite hydrogels carrying growth factor for wound healing. Mater Sci Eng C 112:110923. https://doi.org/10.1016/j.msec.2020.110923
18. Liu B, Yao T, Ren L, Zhao Y, Yuan X (2018) Antibacterial PCL electrospun membranes containing synthetic polypeptides for biomedical purposes. Colloids Surf B: Biointerfaces 172:330–337. https://doi.org/10.1016/j.colsurfb.2018.08.055
19. Xi Y, Song T, Tang S, Wang N, Du J (2016) Preparation and antibacterial mechanism insight of polypeptide-based micelles with excellent antibacterial activities. Biomacromol 17:3922–3930. https://doi.org/10.1021/acs.biomac.6b01285
20. Liu J, Xu Y, Lin X, Ma N, Zhu Q, Yang K, Li X, Liu C, Feng N, Zhao Y, Li X, Zhang W (2023) Immobilization of poly-L-lysine brush via surface initiated polymerization for the development of long-term antibacterial coating for silicone catheter. Colloids Surf B Biointerfaces 221:113015. https://doi.org/10.1016/j.colsurfb.2022.113015
21. Tang C-C, Zhang S-H, Phan THM, Tseng Y-C, Jan J-S (2021) Block length and topology affect self-assembly and gelation of poly(l-lysine)-*block*-poly(S-benzyl-l-cysteine) block copolypeptides. Polymer 228:123891. https://doi.org/10.1016/j.polymer.2021.123891
22. Chen Y-F, Shiau A-L, Chang S-J, Fan N-S, Wang C-T, Wu C-L, Jan J-S (2017) One-dimensional poly(L-lysine)-*block*-poly(L-threonine) assemblies exhibit potent anticancer activity by enhancing membranolysis. Acta Biomater 55:283–295. https://doi.org/10.1016/j.actbio.2017.04.009
23. Chen Y-F, Chang C-H, Hsu M-W, Chang H-M, Chen Y-C, Jiang Y-S, Jan J-S (2020) Peptide fibrillar assemblies exhibit membranolytic effects and antimetastatic activity on lung cancer cells. Biomacromol 21:3836–3846. https://doi.org/10.1021/acs.biomac.0c00911
24. Tsai Y-L, Tseng Y-C, Chen Y-M, Wen T-C, Jan J-S (2018) Zwitterionic polypeptides bearing carboxybetaine and sulfobetaine: synthesis, self-assembly, and their interactions with proteins. Polym Chem 9:1178–1189. https://doi.org/10.1039/C7PY01167A
25. Hou S-S, Fan N-S, Tseng Y-C, Jan J-S (2018) Self-assembly and hydrogelation of coil-sheet poly (L-lysine)-*block*-poly (L-threonine) block copolypeptides. Macromolecules 51:8054–8063. https://doi.org/10.1021/acs.macromol.8b01265
26. Shen X-Y, Tang C-C, Jan J-S (2018) Synthesis and hydrogelation of star-shaped poly (L-lysine) polypeptides modified with different functional groups. Polymer 151:108–116. https://doi.org/10.1016/j.polymer.2018.07.051
27. Chen B-Y, Huang Y-C, Jan J-S (2015) Molecular assembly of alkyl chain-grafted poly (L-lysine) tuned by backbone chain length and grafted alkyl chain. RSC Adv 5:22783–22791. https://doi.org/10.1039/C4RA14290J
28. Chen B-Y, Huang Y-F, Huang Y-C, Wen T-C, Jan J-S (2014) Alkyl chain-grafted poly (l-lysine) vesicles with tunable molecular assembly and membrane permeability. ACS Macro Lett 3:220–223. https://doi.org/10.1021/mz4005327
29. Holowka EP, Sun VZ, Kamei DT, Deming TJ (2007) Polyarginine segments in block copolypeptides drive both vesicular assembly and intracellular delivery. Nat Mater 6:52–57. https://doi.org/10.1038/nmat1794
30. Sun J, Chen X, Deng C, Yu H, Xie Z, Jing X (2007) Direct formation of giant vesicles from synthetic polypeptides. Langmuir 23:8308–8315. https://doi.org/10.1021/la701038f
31. Jung SJ, Park MH, Moon HJ, Ko DY, Jeong B (2014) Thermal gelation or gel melting: (ethylene glycol)113-(l-alanine)12 and (ethylene glycol)113-(l-lactic acid)12. J Polym Sci Part A: Polym Chem 52:2434–2441. https://doi.org/10.1002/pola.27254
32. Zhang Y, Lu H, Bargmann CI (2005) Pathogenic bacteria induce aversive olfactory learning in Caenorhabditis elegans. Nature 438:179–184. https://doi.org/10.1038/nature04216
33. Kuo CJ, Wang ST, Lin CM, Chiu HC, Huang CR, Lee DY, Chang GD, Chou TC, Chen JW, Chen CS (2018) A multi-omic analysis reveals the role of fumarate in regulating the virulence of enterohemorrhagic Escherichia coli. Cell Death Dis 9:381. https://doi.org/10.1038/s41419-018-0423-2

## Authors and Affiliations

**Ying-Jung Cheng[1] · Yi-Sheng Jiang[1] · Cheng-Rung Huang[2] · Chang-Shi Chen[2] · Jeng-Shiung Jan[1,3]**

✉ Jeng-Shiung Jan
jsjan@mail.ncku.edu.tw

Ying-Jung Cheng
yinglongcheng@gmail.com

Yi-Sheng Jiang
js3794490@gmail.com

Cheng-Rung Huang
jackie31428@gmail.com

Chang-Shi Chen
cschen@mail.ncku.edu.tw

[1] Department of Chemical Engineering, National Cheng Kung University, No. 1, University Rd., East Dist., Tainan 70101, Taiwan

[2] Department of Biochemistry and Molecular Biology, College of Medicine, National Cheng Kung University, Tainan, Taiwan

[3] Program On Smart and Sustainable Manufacturing, Academy of Innovative Semiconductor and Sustainable Manufacturing, National Cheng Kung University, Tainan 70101, Taiwan